International Journal of Nanomedicine

Dovepress
open access to scientific and medical research

Open Access Full Text Article

ORIGINAL RESEARCH

Targeted delivery of polypeptide nanoparticle for treatment of traumatic brain injury

This article was published in the following Dove Press journal:
International Journal of Nanomedicine

Peng Wu[1]
Haitian Zhao[2]
Xingchun Gou[3]
Xingwang Wu[4]
Shenqi Zhang[1]
Gang Deng[1]
Qianxue Chen[1]

[1]Department of Neurosurgery, Renmin Hospital of Wuhan University, Wuhan, Hubei 430060, People's Republic of China; [2]School of Chemistry and Chemical Engineering, Harbin Institute of Technology, Harbin, 150001, People's Republic of China; [3]Shaanxi Key Laboratory of Brain Disorders & Institute of Basic and Translational Medicine, Xi'an Medical University, Xi'an 710021, People's Republic of China; [4]Department of Radiology, The First Affiliated Hospital of Anhui Medical University, Hefei, Anhui, 230020, People's Republic of China

Background and purpose: Traumatic brain injury (TBI) is a major disease without effective treatment. Recently, Tat-NR2B9c peptide emerged as a promising neuroprotective agent, but limited in clinical translation by it low brain penetrability. We synthesized Tat-NR2B9c loaded self-assembled activatable protein nanoparticles, termed TN-APNPs, and demonstrated that TN-APNPs enhanced the delivery of Tat-NR2B9c to the brain lesion in stroke. Herein we developed a novel approach to further engineering TN-APNPs for targeted delivery of Tat-NR2B9c to the injured brain with enhanced efficiency through conjugation of CAQK or CCAQK, a short peptide.

Methods: Short peptide-conjugated TN-APNPs were synthesized by conjugated with CAQK or CCAQK via a click condensation reaction with CBT, then analyzed by dynamic light scattering, transmission electron microscopy and thrombin responsive assay. Characterization of short peptide-conjugated TN-APNPs were investigated by using cell excitotoxicity assay and transwell blood-brain-barrier model in vitro, and pharmacokinetics, IVIS imaging system and confocal analysis in TBI-bearing mice. Evaluation of therapeutic effects were analyzed by H&E staining, Elevated Plus Maze analysis and Rotarod test.

Results: CAQK-conjugated TN-APNPs (C-TN-APNPs) and CCAQK-conjugated TN-APNPs (CC-TN-APNPs) were spherical in morphology and 30 nm in diameter. In vitro studies revealed that TN-APNPs, C-TN-APNPs and CC-TN-APNPs were responsive to thrombin cleavage, reduced the cytotoxicity of Tat-NR2B9c, and increased BBB permeability of Tat-NR2B9c. CC-TN-APNPs demonstrated the better circulation time, better targeting ability and penetrating efficiency to the injured brain, and better therapeutic benefits in vivo studies.

Conclusion: This study demonstrated CC-TN-APNPs as a promising therapeutic for clinical management of TBI.

Keywords: traumatic brain injury, Nanoparticle, Tat-NR2B9c, CAQK, CCAQK

Introduction

Due to its high disability and mortality rate, traumatic brain injury (TBI) is a growing public health challenge around the world. Many survivors experience a series of complications, which may lead to a low-quality life with a large economic and psychological burden.[1] TBI is characterized by a primary impact injury, which is mechanical damage to brain tissue at the time of trauma. Successive secondary injury, which is induced by the primary injury, may result from a variety of pathophysiological processes, including neuroinflammation, excitotoxicity, and oxidative damage,[2] and may result in mental disorders, neurodegenerative diseases, and death. Therefore, the ultimate goal for TBI treatment is not only the prevention

Correspondence: Qianxue Chen
Department of Neurosurgery, Renmin Hospital of Wuhan University, Wuhan, Hubei 430060, People's Republic of China
Email chenqx666@whu.edu.cn

submit your manuscript | www.dovepress.com
DovePress
http://doi.org/10.2147/IJN.S202353

and treatment of primary injury but also the retrieval and restoration of neurofunction by relief of secondary injury.

N-methyl-D-aspartate receptor (NMDAR) is an ionotropic glutamate receptor, which plays an important role in both normal development and function of the central nervous system (CNS), and neurological disorders post-injury.[3] Reducing the NMDAR-mediated excitotoxicity is one therapeutic strategy for treating secondary injury in both TBI and stroke.[4] Postsynaptic density-95 (PSD-95) is a prominent organizing protein that couples to NMDAR linking them to downstream neurotoxic signaling molecules.[5] To inhibit PSD-95, a 20-amino acid peptide, Tat-NR2B9c was designed to interfere with the NMDAR-PSD-95 interaction, and prevent neuronal death successfully at rodent animals.[6] Same promising results were found in non-human primates experiments.[7] Furthermore, Tat-NR2B9c was tested in a phase 2 clinical trial (ENACT) for its efficacy on reducing ischemic brain damage in patients undergoing endovascular repair of a brain aneurysm. There were no serious adverse events found to be associated with Tat-NR2B9c treatment in the ENACT clinical trial, although some limited but promising neuroprotective results were shown.[8] The limited efficacy is likely due to the limited brain penetrability of Tat-NR 2B9c. In addition to poor instability and short half-life of free peptides, Tat-NR2B9c may penetrate biological membranes without selectivity, and thus non-specifically binds to cells or organs during circulation.[9,10] Consequently, only a limited amount of Tat-NR2B9c reaches the brain.

Recently, we developed Tat-NR2B9c-loaded self-assembling activatable protein nanoparticles (TN-APNPs) and demonstrated that intravenous administration of TN-APNPs effectively improves the recovery of stroke-bearing mice.[10] In this study, we set to further engineer TN-APNPs for targeted delivery of Tat-NR2B9c to the brain for TBI treatment through surface conjugation of CAQK, a four-amino acid peptide that was reported to have high affinity with extracellular matrix at the site of injured brain.[11] The N-terminal cysteine is likely important for the targeting effect of CAQK. To avoid reducing the function of CAQK, we also synthesized and evaluated TN-APNPs with conjugation of CCAQK. The resulting CAQK and CCAQK conjugated TN-APNPs, designated as C-TN-APNPs and CC-TN-APNPs, respectively, were evaluated in the controlled cortical impact (CCI) mouse model. We found that compared to C-TN-APNPs, CC-TN-APNPs demonstrated greater brain penetrability and blood circulation. We further showed that intravenous administration of CC-TN-APNPs effectively improved the recovery of TBI-bearing mice.

Materials and methods

Materials and cell culture

All chemicals and materials were supplied by Sigma-Aldrich unless otherwise specified. MAL-PEG2000-NHS and MAL-PEG2000-NH_2 were obtained from JenKem Technology. All cells were purchased from American Type Culture Collection (ATCC, Manassas, VA). Human brain microvascular endothelial (hCMEC/D3) cells were grown in EGM, and NHA cells were grown in DMEM supplemented with 10% FBS.[12] SH-SY5Y cells were grown in DMEM-F12 supplemented with 10% FBS and differentiated in Neurobasal medium supplemented with B-27 under 10 μM all-trans retinoic acid (ATRA) condition.[13] All culture medium contained 1% penicillin-streptomycin solution. All culture medium and supplements were purchased from Thermo Fisher Scientific.

Preparation of peptide-conjugated TN-APNPs

TN-APNPs were synthesized according to our previously reported procedures,[10] except MAL-PEG2000-CBT, instead of MAL-PEG2000-NH_2, was used. MAL-PEG 2000-CBT was obtained by reacting MAL-PEG2000-NHS with 2x mole excess of CBT. For peptide conjugation, CAQK or CCAQK (2:1 mole ratio to the CBT group) was added to TN-APNPs and reacted via CBT-Cys click reaction.[14] After 1-hr reaction, unreacted peptides were removed through dialysis in PBS solution for use and stock. NPs concentration was determined with the BCA kit (Sigma Aldrich).

Dynamic light scattering (DLS) and transmission electron microscopy (TEM)

Nanoparticles (NPs) were prepared in PBS (pH 7.4) at a concentration of 50 μg/mL and filtered before measurement, which was carried out using a ZetaSizer Nano ZEN 5600 (Malvern). Mean hydrodynamic diameters were described as Z-average (±SD) (d.nm). Predicted molecular weights were described as kDa. TEM samples were prepared in ddH_2O at a concentration below 50 μg/mL, filtered and then applied to holey carbon-coated copper grids (SPI, West Chester, PA, USA). The grid was placed on a droplet of sample solution (8 μL) for 10 mins. Samples

were imaged using a TEM microscope (FEI Tecnai TF20 TEM).

Thrombin responsive assay

NPs were subjected to thrombin treatment at room temperature according to the method described in our previous research.[10] Changes in the size and morphology were determined by DLS and TEM.

Cell excitotoxicity assay

SH-SY5Y cells were seeded and differentiated to mimic neuron[13] in 0.001% Poly-L-lysine pre-coated 96-well plates at a density of 10^4 cells per well. For the cell excitotoxicity assay, 200 μM of NPs were added to culture medium. After 48 hrs, the cells were subjected to the standard MTT assay.[10]

In vitro transwell blood–brain barrier (BBB) model

The transwell BBB model was established as previously reported.[12] Briefly, transwell inserts were pre-coated with 0.001% Poly-L-lysine, then NHA cells were seeded to the basolateral side of the inserts. The insert was inverted after 4–5 hrs. hCMEC/D3 cells were seeded on the apical side on the second day. The model was considered mature when trans-endothelial electrical resistance (TEER) values reached 30 Ω*cm^2. To simulate BBB leakage, the model was treated with 500 μM $CoCl_2$ for 24 hrs. The medium was refreshed and equal concentrations of FITC-conjugated NPs, diluted with EGM, were added to the apical side of the inserts. The basolateral side was filled with 700 μL of complete DMEM. At time intervals from 30 mins to 72 hrs, samples were taken from the basolateral side to detect FITC intensity with a microplate reader (Synergy™ Mx, BioTek Instruments, Inc.).

Animals

All animal experiments were approved by the Institutional Animal Care and Use Committee at Renmin Hospital of Wuhan University, according to Laboratory animal—Guideline for ethical review of animal welfare (GB/T 35892–2018). C57BL/6 male mice with weight of around 25 g each were given free access to food and water under 12/12-hr light and dark cycle, and allowed to acclimate for 1 week prior to procedures for recovery from transportation-related stress.

Controlled cortical impact (CCI) model of TBI in mice

Mice were anesthetized with 5% isoflurane (2% for maintenance) and securely positioned in the stereotaxic frame. Fur on the top of the skull was shaved, and the surgical site was disinfected with povidone-iodine solution and then twice with isopropanol. An approximately 10-mm midline scalp incision was made to expose the right parietal cortex. A 3-mm cranial window was made in the skull over the right cortex (bregma as central, and antero-posterior −3 mm, medio-lateral +1 mm, dorso-ventral 1 mm) using a surgical trephine drill. Extreme care was taken to avoid damage to the dura. The controlled cortical impactor (Leica Impactor One) was attached to the stereotaxic frame with a 2-mm impactor tip and was used to impact the dura. The controlled impact parameters were: velocity 3 m/s, depth 1 mm, and dwell time 85 ms. After bleeding stopped, a thin piece of bone wax was used to cover the craniotomy and the skin was sutured.

Characterization of pharmacokinetics

NPs were conjugated with equal mole of Alex Flour 750 (AF750) through reaction with AF750 NHS Ester (ThermoFisher Scientific) in PBS (pH 7.4). Unreacted dye was removed through dialysis. NPs were injected via the tail vein 10 mins after CCI surgery (n=5 mice per group). Each group blood (20 μL) was collected at 5, 15, 30 mins and 1, 3, 6, 12, 24, 36, 48 hrs after injection using a heparinized pipette. Blood was stored in an EP tube with 20 μL heparin (50 U/mL), mixed, and centrifuged at 3,000 g for 10 mins at 4°C. The plasma was collected after centrifuge. Plasma AF750 concentration was quantified based on AF750 fluorescence and plotted with time. Fluorescence intensity was detected immediately with a microplate reader (Synergy™ Mx, BioTek Instruments, Inc.).

Characterization of NP delivery to the brain

Alex Flour 750-conjugated NPs were prepared as described earlier and injected through a tail vein immediately after surgery. Five mice were used in each group. After 24 hrs, the mice were sacrificed, and the brains were isolated and subjected to imaging using an IVIS imaging system (Caliper, CA). The fluorescence intensity was quantified using a Living Image 3.0 (Caliper, CA). The interaction of PSD-95 and Tat-NR2B9c, which released from CC-TN-APNPs, was investigated as previously

described. Images were captured using a laser scanning confocal microscope (Leica TCS SP8).[10]

Neurological evaluation in TBI mice model

Injured area was determined by H&E staining. Size of brain injury was analyzed by using Image J (ver. 1.51k). Anxiety was quantified by using an Elevated Plus Maze analysis instrument (EPM) at 2 weeks post CCI surgery. Motor function was determined by using the Rotarod test at 2 weeks post CCI surgery. EPM analysis and Rotarod test were performed as described previously.[15–17] Briefly, for EPM analysis, mice were placed on the center platform and face to the open arm, then collected data for 5 mins. Time, distance, and entrance of open arms/close arms were collected, and anxiety index was calculated by using this equation: anxiety index = $\text{time}_{(\text{open arms})}/\text{time}_{(\text{total time})}$. For Rotarod test, mice were placed on the rotating beam at 4 rpm for 1 min, then increase the speed further to 40 rpm in 5 mins and leave mice in place for a further 2 mins. Falling speed and falling time were collected. All tests were repeated three times. All mice were trained daily for 3 days prior to CCI surgery (n=5 mice per group) and given a 15mins break between each tests. Sham animals received the craniotomy described for CCI surgery without impaction and were treated with PBS injection. Control animals received surgery and were treated with PBS injection.

Data analysis

Data were expressed as means ± SEM. To determine the difference among groups, data were analyzed by one-way ANOVA followed by Tukey's multiple comparison tests and performed by histogram, or two-way ANOVA followed by Bonferroni's post-tests and performed by line chart. Statistics were performed using GraphPad Prism version 5.00 (GraphPad Software, La Jolla California USA). Significance level was set at *P<0.05 for all these analyses.

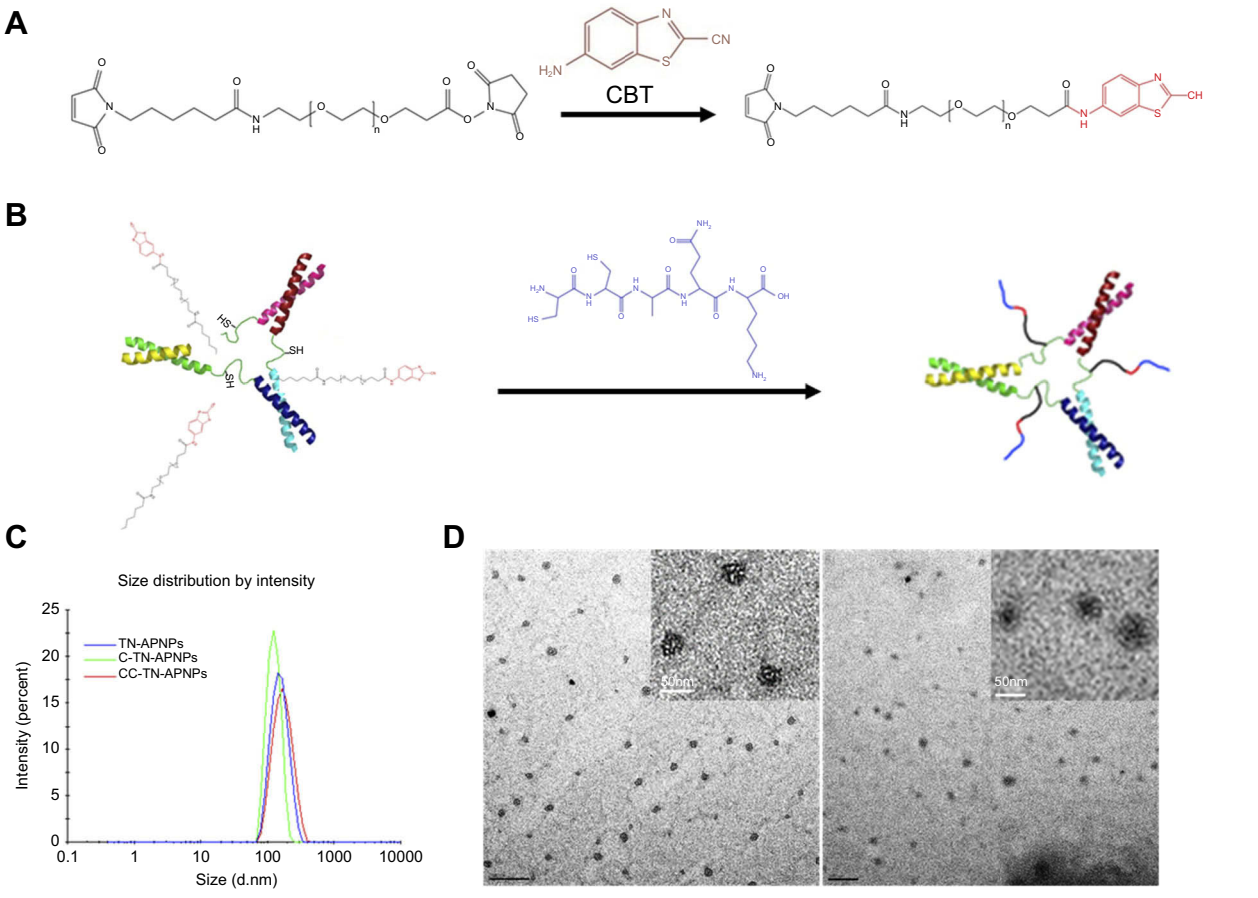

Figure 1 Synthesis of peptide-conjugated TN-APNPs. (**A**) Schematic diagram of synthesis of MAL-PEG2000-CBT. (**B**) Schematic diagram of conjugation of CCAQK peptides to TN-APNPs. (**C**) DLS analysis of TN-APNPs with and without peptide conjugation. (**D**) Representative TEM images of CC-TN-APNPs (left) and C-TN-APNPs (right) (white scale bar, 50 nm).

Results and discussion

Synthesis and characterization of peptide-conjugated TN-APNPs

To enhance targeted delivery of TN-APNPs, we developed a strategy to conjugate CAQK (Figure 1A and B), a peptide that was previously reported to enhanced drug delivery to the injured brain.[11] As we could not exclude the possibility that the N-terminal cysteine is important for the targeting effect, we also synthesized TN-APNPs that were conjugated with CCAQK. First, we generated MAL-PEG2000-CBT by reacting MAL-PEG2000-NHS with CBT (Figure 1A). The resulting MAL-PEG2000-CBT was used in the synthesis of TN-APNPs by replacing MAL-PEG2000-NH_2 according to our recent report.[10] As the last step, the selected peptide was conjugated to TN-APNPs through reaction with the cyano group in CBT (Figure 1B), which interacts with N-terminal cysteine via a click condensation reaction.[14] The obtained peptide-conjugated TN-APNPs were characterized by DLS and TEM. DLS analysis showed that the hydrodynamic diameter sizes were 146±50 nm for TN-APNPs, 120±20 nm for CAQK-conjugated TN-APNPs (C-TN-APNPs), and 159±50 nm for CCAQK-conjugated TN-APNPs (CC-TN-APNPs) (Figure 1C). TEM analysis revealed that both the C-TN-APNPs and CC-TN-APNPs were spherical in morphology and in diameter of 30 nm (Figure 1D).

In vitro characterization of peptide-conjugated TN-APNPs

As described in our recent report,[10] TN-APNPs were developed for delivery of Tat-NR2B9c to the ischemic region in the brain, where the locally enriched thrombin cleaved TN-APNPs and released Tat-NR2B9c. Similarly, the level of thrombin is known to be elevated in the injured region of the brain with TBI.[18] To determine if the peptide-conjugated TN-APNPs were responsive to thrombin cleavage, we treated C-TN-APNPs and CC-TN-APNPs with thrombin. We found that, similar to the finding for TN-APNPs,[10] thrombin treatment efficiently degraded both C-TN-APNPs and CC-TN-APNPs, as determined by DLS analysis (Figure 2A, Figure S1A) and TEM imaging (Figure 2B, Figure S1B).

We determined the potential neuronal toxicity of C-TN-APNPs and CC-TN-APNPs. Neuron-like cells were obtained through differentiation of SH-SY5Y cells with ATRA treatment, due to SH-SY5Y cells can be differentiated to a more mature neuron-like phenotype that is char-

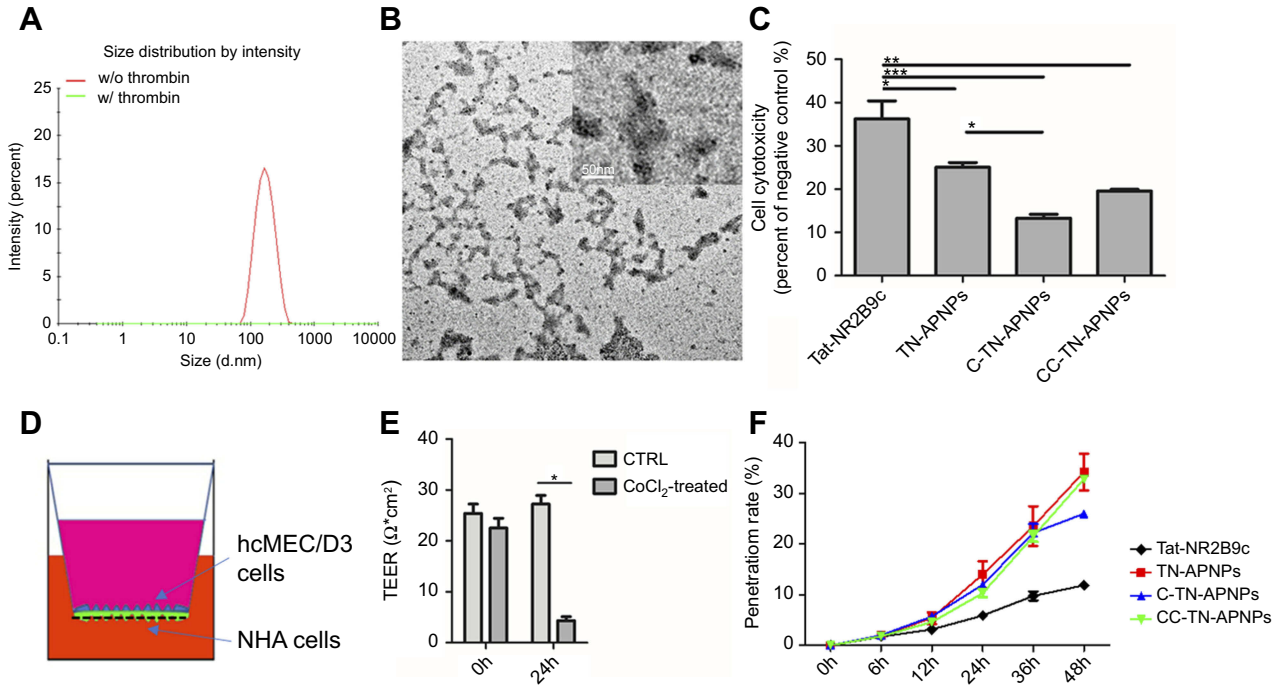

Figure 2 In vitro characterization of TN-APNPs with and without peptide conjugation. (**A**) DLS analysis of CC-TN-APNPs with and without treatment of thrombin. (**B**) Representative TEM images of CC-TN-APNPs after thrombin treatment (scale bar, 50 nm). (**C**) Cytotoxicity of Tat-NR2B9c (200 nM) and TN-APNPs with and without peptide conjugation (200 nM equivalent dose of Tat-NR2B9c), repeat three times. (**D**) Schematic diagram of in vitro BBB model. (**E**) Quantification of TEER value with and without $CoCl_2$ treatment. (**F**) BBB penetrability of Tat-NR2B9c and the indicated NPs. *P<0.05, **P<0.01, ***P<0.001.

acterized by neuronal markers, and propagated.[13] Results in Figure 2C show that, compared to free Tat-NR2B9c peptide, TN-APNPs exhibited less toxicity, and conjugation of peptide further reduced the toxicity of TN-APNPs. We supposed that this interesting phenomenon might cause by slightly change of space structures and surface molecule.

The BBB, which is partially disrupted after traumatization, remains as the major impediment for systemic treatment of TBI.[19,20] We assessed if conjugation of peptides enhances the ability of TN-APNPs to penetrate the compromised BBB by using an in vitro BBB model, which was established by culturing hCMEC/D3 cells on the top and astrocyte NHA cells at the bottom of the insert membrane (Figure 2D). Disruption of the BBB was induced by adding $CoCl_2$ as previously reported[21] and confirmed by quantification of transepithelial/transendothelial electrical resistance (TEER) values (Figure 2E). We found that all NPs, including TN-APNPs, C-TN-APNPs, and CC-TN-APNPs, demonstrated a high degree of BBB permeability, which is significantly greater than that of free Tat-NR2B9c peptide (Figure 2F). This phenomenon may relate the cell endocytosis and exocytosis, or nanoparticles form help drug to escape intracellular lyase.

Characterization of peptide-conjugated TN-APNPs in TBI-bearing mice

We evaluated if conjugation of peptides enhanced the accumulation of NPs in the injured brain. TBI-bearing mice were established through CCI surgery. Ten minutes after surgery, mice received intravenous administration of AF750 conjugated TN-APNPs, C-TN-APNPs, or CC-TN-APNPs. The doses of NPs were normalized based on the fluorescence intensity of AF750 to ensure that each mouse received the same amount of fluorescence. After 24 hrs, the mice were euthanized. The brains were harvested and imaged. We found that CC-TN-APNPs demonstrated the greatest efficiency in penetrating the injured brain (Figure 3A). Based on the fluorescence intensity, conjugation of CAQK and CCAQK enhanced the delivery by 1.82 and 2.24 folds, respectively (Figure 3B).

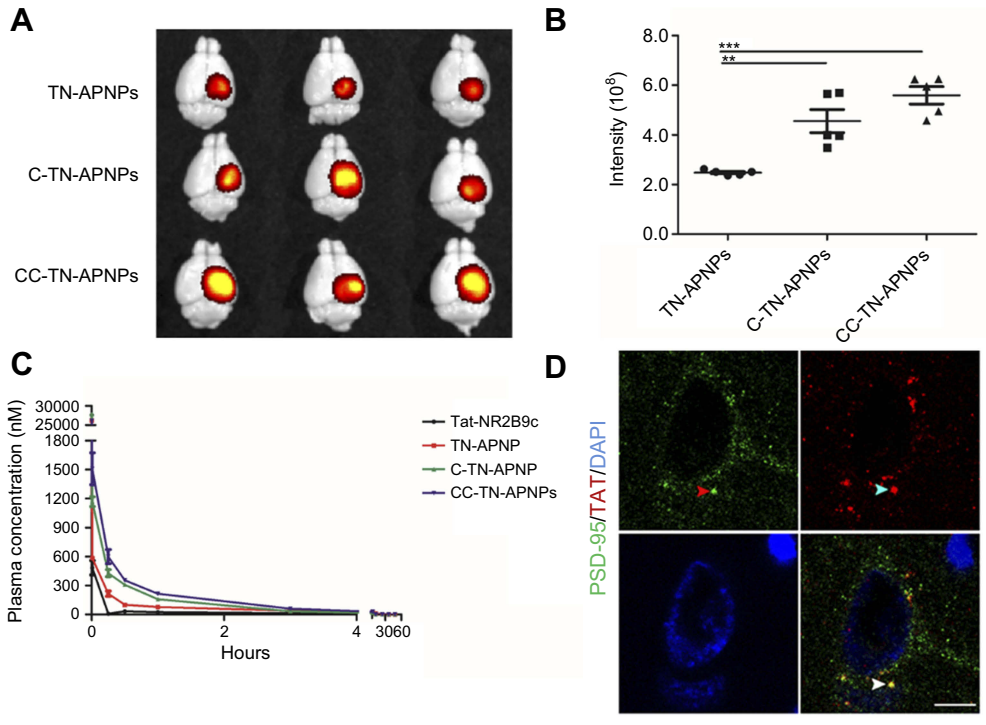

Figure 3 In vivo characterization of NPs. (**A**) Representative images of the brains isolated from mice that received the indicated treatments. (**B**) Semi-quantification of NPs in the excised brains based on AF750 fluorescence intensity. Intensity was quantified using living image 3.0. *P<0.05, **P<0.01, ***P<0.001. (**C**) Blood circulation of Tat-NR2B9c and NPs of the indicated formulations. (**D**) Confocal analysis of the interaction of PSD-95 and Tat-NR2B9c in a representative ipsilateral penumbra. PSD-95 and Tat-NR2B9c were identified by an anti-PSD-95 antibody and an anti-TAT antibody, respectively. Scale bar: 7.5 μm.

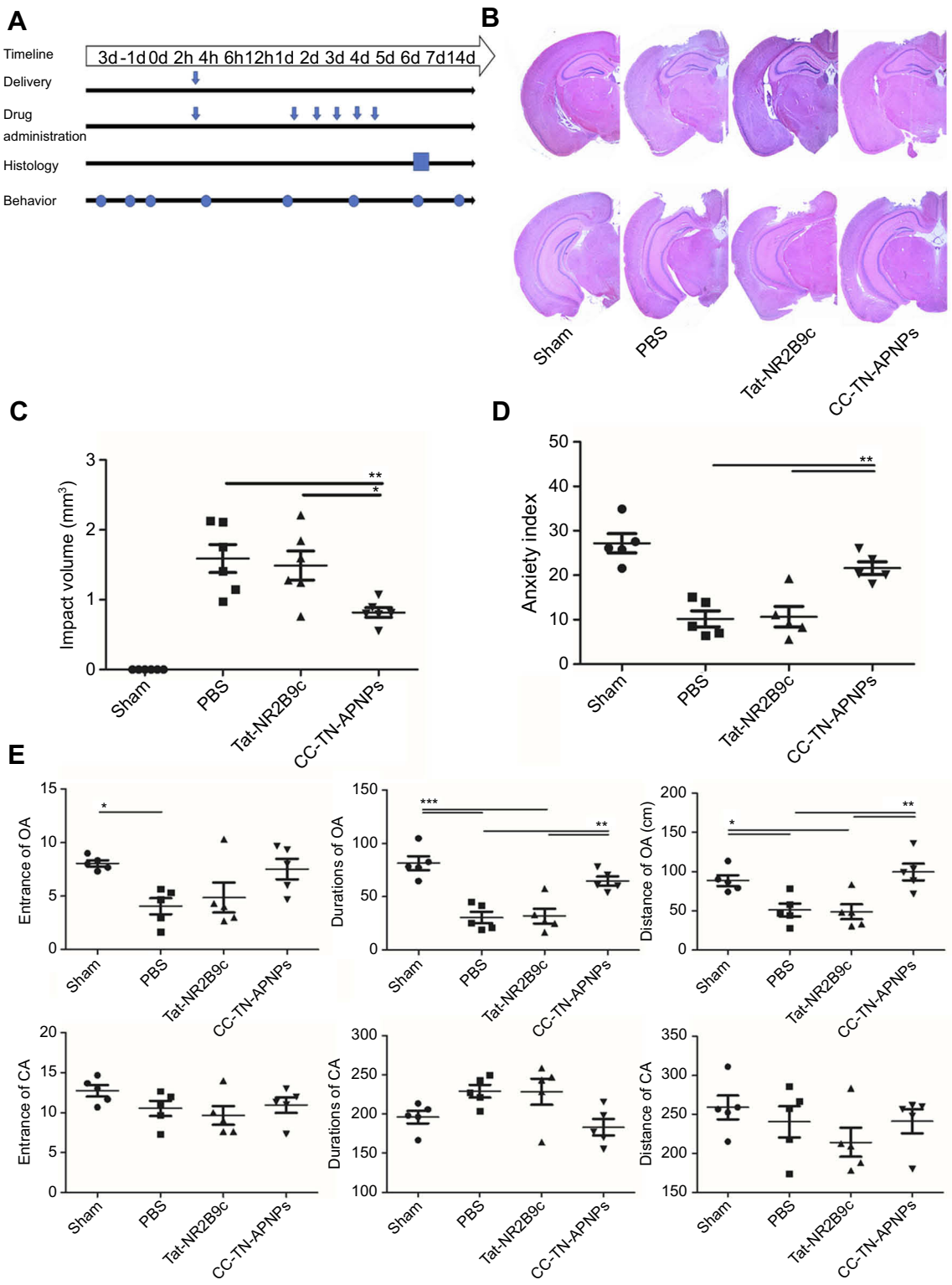

Figure 4 Evaluation of CC-TN-APNPs treatment in CCI mice model. (**A**). Timeline for treatment and evaluation. (**B**) Representative H&E staining images of the brain isolated from mice received the indicated treatment. (**C**) Quantification of the injured volume in mice received the indicated treatment. (**D** and **E**). EPM analysis of mice received the indicated treatment, open arms (OA) or closed arms (CA), and anxiety index. **P*<0.05, ***P*<0.01, ****P*<0.001.

We determined the blood circulation of AF750-conjugated TN-APNPs, C-TN-APNPs, or CC-TN-APNPs in normal mice. Results in Figure 3C showed that, consistent with our previous report,[10] TN-APNPs have significantly greater circulation time than Tat-NR2B9c and, conjugation of peptides further enhanced the circulation of TN-APNPs.

Compared to C-TN-APNPs, CC-TN-APNPs demonstrated greater brain penetrability and blood circulation, and thus were selected for further characterization. We analyzed whether Tat-NR2B9c could be released in the brain and penetrate into cells after delivery via CC-TN-APNPs by immunostaining. Similar to our previous finding with TN-APNPs,[10] confocal analysis of the ipsilateral penumbra from mice treated with CC-TN-APNPs showed that Tat-NR2B9c was released, penetrated cells, and interacted with its intracellular target PSD-95 (Figure 3D). There wasn't Tat-NR2B9c accumulated in contralateral brain tissue, which have normal BBB without thrombin leakage (Figure S2). Taken together, CC-TN-APNPs have better delivery efficiency, longer circulating time, and the same releasing ability. These advantages indicated that CC-TN-APNPs might achieve better results in treatment of TBI.

Characterization of therapeutic benefit of CC-TN-APNPs for TBI treatment

We assessed CC-TN-APNPs for TBI treatment. Mice were subjected to CCI surgery and randomized into three experimental groups, which received treatment of PBS, free TAT-NR2B9c peptide, and CC-TN-APNPs, respectively. Timeline for treatment and evaluation is shown in Figure 4A. Morphometric analysis of the brain showed that treatment with CC-TN-APNPs reduced the injury size by Image J (version 1.51, NIH, USA). The range of measurement was shown in Figure S3. In contrast, treatment with the same amount of free Tat-NR2B9c peptide fails to achieve a comparable effect (Figure 4B and C). Anxiety, dysphoria, and aggression are hallmarks of post-traumatic stress disorder, which is a common comorbidity in TBI.[22] Elevate Plus Maze (EPM) test found that, compared to those mice treated with PBS or free Tat-NR2B9c, the mice treated with CC-TN-APNPs showed significantly less anxiety, dysphoria, and appeared to be less aggressive, and more motivated to discover and stay in the open arms (OA) of the EPM instrument (Figure 4D and E). We also performed Rotated test, which failed to detect significant difference in mouse movement ability among different groups, although CC-TN-APNPs treatment group had a slight improvement recovery trend compared to the other groups (Figure S4). This is likely because the injury was not induced in the region close enough to the motor cortex and therefore the recovery was not relevant to those determined by the Rotated test. Taken together, these results suggest that treatment with CC-TN-APNPs is significantly beneficial for recovery after TBI.

Conclusion

In this study, we engineered TN-APNPs for targeted delivery of TAT-NR2B9c peptide to the injured brain through conjugation of short peptide for TBI treatment. We synthesized and characterized two engineered TN-APNPs, including C-TN-APNPs and CC-TN-APNPs, and found that CC-TN-APNPs demonstrated the greater brain targeting efficiency. We characterized CC-TN-APNPs in TBI mice that were induced by CCI surgery and found that intravenous administration of CC-TN-APNPs effectively reduced the injury size and significantly improved the psychological outcomes. Due to its simple formulation and significant therapeutic effect, CC-TN-APNPs may be translated into clinical application for clinical management of TBI.

Acknowledgments

This work was supported by National Natural Science Foundation of China (No. 81572489, 81372683, and 81502175) and Projects of International Cooperation and Exchanges Natural Science Foundation of Shannxi Province of China (no. 2018KW-038) .

Disclosure

The authors report no conflicts of interest in this work.

References

1. Maas AIR, Menon DK, Adelson PD, et al. Traumatic brain injury: integrated approaches to improve prevention, clinical care, and research. *Lancet Neurol*. 2017;16(12):987–1048. doi:10.1016/S1474-4422(17)30371-X
2. Kumar A, Loane DJ. Neuroinflammation after traumatic brain injury: opportunities for therapeutic intervention. *Brain Behav Immun*. 2012;26(8):1191–1201. doi:10.1016/j.bbi.2012.06.008
3. Haberny KA, Paule MG, Scallet AC, et al. Ontogeny of the N-methyl-D-aspartate (NMDA) receptor system and susceptibility to neurotoxicity. *Toxicol Sci*. 2002;68(1):9–17. doi:10.1093/toxsci/68.1.9
4. Parsons MP, Raymond LA. Extrasynaptic NMDA receptor involvement in central nervous system disorders. *Neuron*. 2014;82(2):279–293. doi:10.1016/j.neuron.2014.03.030
5. Cui H, Hayashi A, Sun HS, et al. PDZ protein interactions underlying NMDA receptor-mediated excitotoxicity and neuroprotection by PSD-95 inhibitors. *J Neurosci*. 2007;27(37):9901–9915. doi:10.1523/JNEUROSCI.1464-07.2007
6. Aarts M, Liu Y, Liu L, et al. Treatment of ischemic brain damage by perturbing NMDA receptor- PSD-95 protein interactions. *Science*. 2002;298(5594):846–850. doi:10.1126/science.1072873
7. Cook DJ, Teves L, Tymianski M. A translational paradigm for the preclinical evaluation of the stroke neuroprotectant Tat-NR2B9c in gyrencephalic nonhuman primates. *Sci Transl Med*. 2012;4(154):154ra133. doi:10.1126/scitranslmed.3003824

8. Hill MD, Martin RH, Mikulis D, et al. Safety and efficacy of NA-1 in patients with iatrogenic stroke after endovascular aneurysm repair (ENACT): a phase 2, randomised, double-blind, placebo-controlled trial. *Lancet Neurol*. 2012;11(11):942–950. doi:10.1016/S1474-4422(12)70225-9
9. Papadopoulou LC, Tsiftsoglou AS. The potential role of cell penetrating peptides in the intracellular delivery of proteins for therapy of erythroid related disorders. *Pharmaceuticals*. 2013;6(1):32–53. doi:10.3390/ph6010032
10. Yu X, Gou X, Wu P, et al. Activatable protein nanoparticles for targeted delivery of therapeutic peptides. *Adv Mater*. 2018;30(7). doi:10.1002/adma.201803888
11. Mann AP, Scodeller P, Hussain S, et al. A peptide for targeted, systemic delivery of imaging and therapeutic compounds into acute brain injuries. *Nat Commun*. 2016;7:11980. doi:10.1038/ncomms11980
12. Czupalla CJ, Liebner S, Devraj K. In vitro models of the bloodʙAVBrain barrier. In: Milner R, editor. *Cerebral Angiogenesis: Methods and Protocols*. New York: Springer New York; 2014:415–437.
13. Kovalevich J, Langford D. Considerations for the use of SH-SY5Y neuroblastoma cells in neurobiology. *Methods Mol Biol*. 2013;1078:9–21. doi:10.1007/978-1-62703-640-5_2
14. Zheng Z, Chen P, Li G, et al. Mechanistic study of CBT-Cys click reaction and its application for identifying bioactive N-terminal cysteine peptides in amniotic fluid. *Chem Sci*. 2017;8(1):214–222. doi:10.1039/c6sc01461e
15. Hunsberger JG, Newton SS, Bennett AH, et al. Antidepressant actions of the exercise-regulated gene VGF. *Nat Med*. 2007;13(12):1476–1482. doi:10.1038/nm1669
16. Lee AS, Duman RS, Pittenger C. A double dissociation revealing bidirectional competition between striatum and hippocampus during learning. *Proc Natl Acad Sci U S A*. 2008;105(44):17163–17168. doi:10.1073/pnas.0807749105
17. Fasano S, Pittenger C, Brambilla R. Inhibition of CREB activity in the dorsal portion of the striatum potentiates behavioral responses to drugs of abuse. *Front Behav Neurosci*. 2009;3:29. doi:10.3389/neuro.08.048.2009
18. Itsekson-Hayosh Z, Shavit-Stein E, Katzav A, et al. Minimal traumatic brain injury in mice: protease-activated receptor 1 and thrombin-related changes. *J Neurotrauma*. 2016;33(20):1848–1854. doi:10.1089/neu.2015.4146
19. Bharadwaj VN, Nguyen DT, Kodibagkar VD, Stabenfeldt SE. Nanoparticle-based therapeutics for brain injury. *Adv Healthc Mater*. 2018;7. doi:10.1002/adhm.201700668.
20. Chodobski A, Zink BJ, Szmydynger-Chodobska J. Blood-brain barrier pathophysiology in traumatic brain injury. *Transl Stroke Res*. 2011;2(4):492–516. doi:10.1007/s12975-011-0125-x
21. Chatard M, Puech C, Perek N, Roche F. Hydralazine is a suitable mimetic agent of hypoxia to study the impact of hypoxic stress on in vitro blood-brain barrier model. *Cell Physiol Biochem*. 2017;42(4):1592–1602. doi:10.1159/000479399
22. Kaplan GB, Leite-Morris KA, Wang L, et al. Pathophysiological bases of comorbidity: traumatic brain injury and post-traumatic stress disorder. *J Neurotrauma*. 2018;35(2):210–225. doi:10.1089/neu.2016.4953

Supplementary Materials

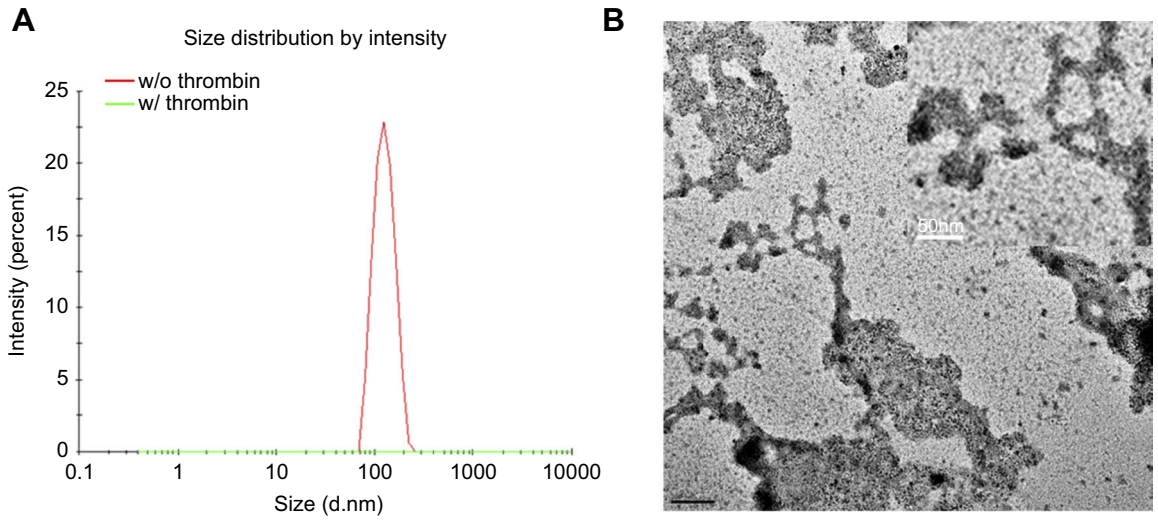

Figure S1 (**A**) DLS analysis of C-TN-APNPs with and without treatment of thrombin. (**B**) Representative TEM images of C-TN-APNPs after thrombin treatment (scale bar, 50 nm).

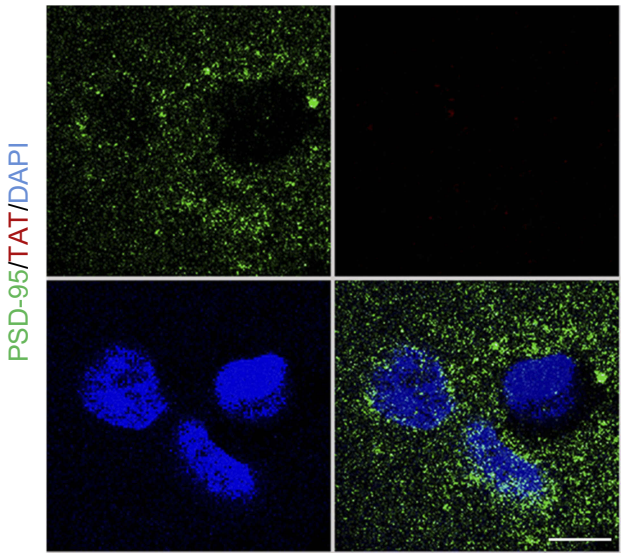

Figure S2 Confocal analysis of the interaction of PSD-95 and Tat-NR2B9c in a representative contralateral non-injury brain tissue. PSD-95 and Tat-NR2B9c were identified by an anti-PSD-95 antibody and an anti-TAT antibody, respectively. Scale bar: 15 μm.

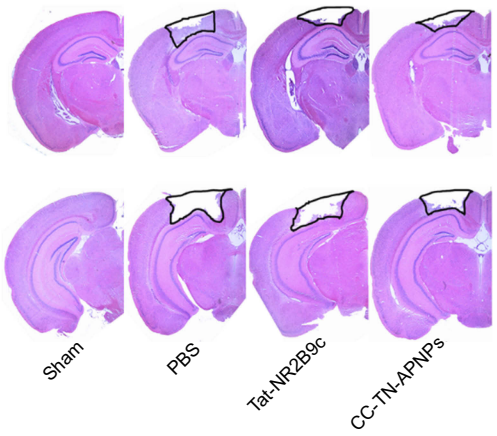

Figure S3 Example for how to calculate impact volume by using Image J software.

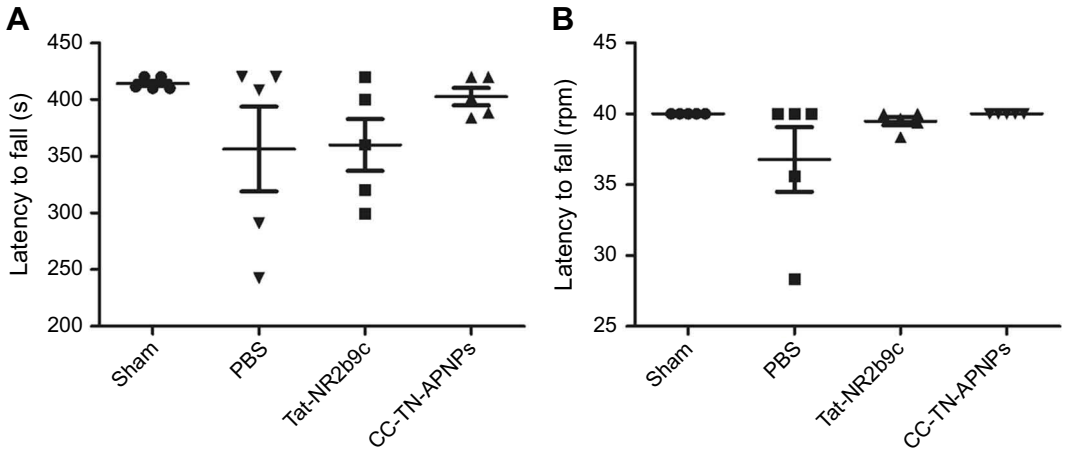

Figure S4 Rotated test of mice received the CC-TN-APNPs treatment (the end points of observation in Rotated test is the mice fall down, the time reach to 420 s or the speed reach to 40 rpm).